

## Advanced Approach for Slopes Measurement by Non - Contact Optical Technique

B. Trentadue

*Dipartimento di Meccanica, Matematica e Management – Politecnico di Bari Viale Japigia 182 – 70126 Bari, Italy*

### ABSTRACT

A numerical computation of a very advanced experimental method to acquire shapes is introduced in this paper. The basic equations that relate the measurement of slopes to the basic geometric and optical parameters of the system are derived. The sensitivity and accuracy of the method are discussed. In order to validate the accuracy and the applicability of this method, the qualitative slope behavior of a loaded metallic layer is given.

**Keywords:** Slope, curvature, optical technique

### I. INTRODUCTION

The moiré reflection method [1] is an optical technique to obtain the slope of reflecting surfaces with very small curvatures. Since its introduction by Lichtenberg, a number of alternate optical arrangements have been proposed to observe the loci of constant projected curvature [2], [3],[4],[5].

This paper presents a new version of reflection moiré. Previous versions have used incoherent illumination and coarse pitch gratings.

### II. OBSERVATION OF SLOPE FRINGES WITH COHERENT ILLUMINATION

The observation of slope fringes requires the projection of a grating, called reference grating, into a control or master grating.

The imaging is done by reflecting the reference grating on a mirror surface whose slope is to be measured.

The moiré fringes produced by the two gratings are the loci of projected constant slope fringes. Since the curvature of a surface is a second order tensor, three components of the tensor must be measured.

The alternative method proposed in this paper uses a well-known phenomenon analyzed in [6].

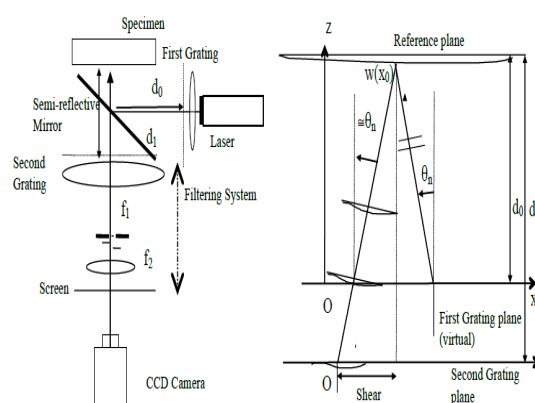


Figure 1: Setup to observe reflection Moiré patterns.

Figure 2: n<sup>th</sup> order path.

When a grating is illuminated with coherent collimated illumination, the grating is reproduced in the space at distances [6],

$$z = \frac{n\lambda}{p^2} \quad (1)$$

where  $z$  is the coordinate perpendicular to the grating,  $p$  is the grating pitch,  $\lambda$  is the wave length of the illumination light and  $n$  is an integer 1,2,3....

Fig. 1 shows one set up that can be used to observe the fringes. The reference grating is projected on the mirror surface whose slope is to be measured by means of a semi-reflecting, semi-transparent

mirror. The moiré pattern is produced by observing the reference grating through the master grating.

In the first method, a translucent screen is located behind the master grating. The observation plane can be changed by adding an optical system and projecting the pattern onto a screen. The sensitivity of the method shows to be dependent on the distance between the mirror surface and the master grating. The location of the master grating must conform with equation (1). In practice, the position of the reference grating is adjusted until maximum visibility fringes are obtained. Fig. 2 shows the optical equivalent of the observation setup.

Two parallel gratings are observed with illumination perpendicular to the grating plane. The normal illumination produces symmetrical optical paths for all the orders that interfere.

The observed fringes depend on the slope of the surface and not on the gap between the two gratings. If the observation is made in the zero order direction, the sequence of orders contributing to the fringes will be given by:

$$r = n - m = 0 \quad (2)$$

Considering an order other than zero, the condition of minimum deviation [7] must be used to obtain symmetrical paths for all the orders so as to observe the patterns obtained. Since the resultant order contains many wave fronts, the resulting fringes are multiple beam interference fringes [7], [8]. As mentioned in [7], the slit and bar type of amplitude modulating gratings under the stated observation conditions will produce fringes that have the fundamental period.

Of course, the presence of the harmonics changes the shape of the fringes. Since the different orders diverge in space, the distance between the two gratings is restricted to values that limit the amount of shearing of the different wave fronts to a reasonable amount.

Essentially, the system is operating as a shear interferometer and the values of the obtained slopes correspond to points whose location is known within the amount of shearing.

### III. DERIVATION OF THE EQUATION OF THE LINES OF CONSTANT SLOPE

This derivation applies to the optical setup shown in Fig. 1. The first grating (Fig. 2) is situated at a distance  $d_0$  from the mirror surface; the second grating is situated at a distance  $d_1$ .

The sum of  $d_0$  and  $d_1$  must satisfy the condition given by equation (1) otherwise they are arbitrary quantities. The phases of wave fronts are referred to the origin of the coordinate system.

The first grating is illuminated in the direction, which is perpendicular to its plane by a plane wave front of wavelength  $\lambda$  and amplitude  $E_0$ .

As this wave front passes through the first grating, it is multiplied by the transmission function of grating 1, thereby producing the different diffraction orders. The angles corresponding to the diffraction orders are given by,

$$\sin \theta_n = \frac{n\lambda}{p} \quad (3)$$

The derivation presented in this paper follows the general lines of the derivation given in [9] for in-plane displacements. In the present case, we are dealing with out-of-plane displacements.

In [9] the combination of the different diffraction orders is discussed in detail and an abbreviated derivation will be given later in this paper.

We will now concentrate on the  $n$ th order shown in Fig.2.

The coordinates system is shown in the same figure.

The origin is taken in the plane of the first grating,  $z$ , increasing as one moves towards the mirror under study.

After the first grating, the wave front is given by:

$$E_n(x, z) = k_n E_0 e^{i\phi_n} e^{i \frac{2\pi}{\lambda} (-x \sin \theta_n + z \cos \theta_n)} = k_n E_0 e^{i\phi_n} e^{-i \frac{2\pi x}{p}} e^{i \frac{2\pi}{\lambda} z \cos \theta_n} \quad (4)$$

where  $\phi_n$  and  $k_n$  are constants for the grating and order considered.

For simplicity, we can consider them relative to the zero order ( $\phi_0=0$  and  $k_0=1$ ).

Reaching the surface, the wave front is:

$$E_n(x_0, d_0 - w(x_0)) \cong k_n E_0 e^{i\phi_n} e^{i2\pi \left( \frac{-nx_0 + d_0 - w(x_0)}{p} \cos\theta_n \right)} \quad (5)$$

Upon reflection on the surface of the object, the wave fronts are rotated by twice the local slope of the object. The reflected wave front is then given by:

$$E_n(x, z) \cong k_n E_0 e^{i\phi_n} e^{i2\pi \left( \frac{-nx_0 + (d_0 - w(x_0))}{p} \cos\theta_n \right)} e^{i2\pi \left( \frac{-(x-x_0) \sin\left(\theta_n + 2\frac{\partial w(x_0)}{\partial x}\right)}{\lambda} + \frac{(d_0 - w(x_0) - z) \cos\left(\theta_n + 2\frac{\partial w(x_0)}{\partial x}\right)}{\lambda} \right)} \quad (6)$$

The second grating is located in plane  $z=d_0-d_1$  therefore, the amplitude incident on the second grating is:

$$E_n(x, d_0 - d_1) \cong k_n E_0 e^{i\phi_n} e^{i2\pi \left( \frac{-x_0 \sin\theta_n + (d_0 - w(x_0)) \cos\theta_n - (x-x_0) \sin\left(\theta_n + 2\frac{\partial w(x_0)}{\partial x}\right)}{\lambda} + \frac{(d_1 - w(x_0)) \cos\left(\theta_n + 2\frac{\partial w(x_0)}{\partial x}\right)}{\lambda} \right)} \quad (7)$$

In Fig. 1 a diaphragm is added that filters all the other orders, except the zero order. Therefore, the only wave fronts that contribute to the pattern have the final order 0. This means that incident order  $+n$  must be rotated back to order  $0=+n-n$ . The final expression of the amplitude in the plane of the second grating for the  $n$ th wave front  $(+n,-n)$  is ( $kn=k-n$  and  $\phi n=\phi-n$ ) for a symmetric grating with transfer function  $T_n^{(2)}(x)$ ,

$$E_{nfinal}(x, d_0 - d_1) = T_n^{(2)}(x) E_n(x, d_0 - d_1) = k_n^2 E_0 e^{i2\phi_n} e^{i\frac{2\pi x}{p}} e^{i\phi_n} e^{i2\pi \left( \frac{-x_0 \sin\theta_n + (d_0 - w(x_0)) \cos\theta_n - (x-x_0) \sin\left(\theta_n + 2\frac{\partial w(x_0)}{\partial x}\right)}{\lambda} + \frac{(d_1 - w(x_0)) \cos\left(\theta_n + 2\frac{\partial w(x_0)}{\partial x}\right)}{\lambda} \right)} \quad (8)$$

where:

$$x_0 = x + d_1 \tan\theta_n \cong x + \frac{nd_1\lambda}{p} \quad (9)$$

Therefore, the phase at point  $x$  in the plane of the second grating depends on the deflection and slope of the surface at a different point ( $x_0$ ). This point differs for each order since its position depends on  $n$ . This will be interpreted as shear interferometry.

Angles  $\left( \frac{\partial w(x)}{\partial x} \right)$  and  $(\theta_n)$  are supposed to be small, and  $\frac{\partial w(x)}{\partial x} < \theta_n$ . Therefore, we can approximate the trigonometric functions:

$$E_n(x, d_0 - d_1) \cong k_n^2 E_0 e^{i2\phi_n} e^{i\frac{2\pi}{\lambda} f(x_0)} \quad (10)$$

This formula gives the wave front coming from the second grating whose order was  $+n$  after the first grating. It is valid for positive or negative values of  $n$ , and shows that the wave fronts are translated combinations of the slope and deflection of the mirror. The wave fronts are sheared.

For the zero order term:

$$E_0(x, d_0 - d_1) \cong E_0 e^{i\frac{2\pi}{\lambda} f(x)} \quad (11)$$

As previously explained, only the zero order light coming from the second grating is collected. This is done by introducing a lens system and filter in the focal plane of the first lens. Consequently, the light distribution observed is the result of interference between all wave fronts with order 0 after the two gratings:  $(+n,-n)$ .

Combining all contributions:

$$E_T(x) = E_0 e^{i\frac{2\pi(d_0+d_1)}{\lambda}} \sum_{n=-N}^N k_n^2 e^{i2\phi_n} e^{i\frac{2\pi}{\lambda} \left( f(x+d_1 \frac{n\lambda}{p}) \right)} \quad (12)$$

Where  $N$  is the highest diffraction order reaching the second grating.

The intensity measured is:

$$I_T(x) = E_T(x) \overline{E_T(x)}$$

$$= E_0^2 \sum_{n=-N}^N \sum_{m=-N}^N k_n^2 k_m^2 e^{i2(\phi_n - \phi_m)} e^{i\frac{2\pi}{\lambda} \left( f(x+d_1 \frac{n\lambda}{p}) - f(x+d_1 \frac{m\lambda}{p}) \right)}$$
(13)

Each term corresponds to shear interference of wave fronts whose phase is given by  $f(x)$ .

We use the first order approximation for  $f(x)$ :

$$f(x + \Delta x) \cong f(x) + \Delta x \frac{\partial f(x)}{\partial x}$$
(14)

Each term is a complex number, but considering the ranges for  $n$  and  $m$ , each term has its conjugate and they recombine to give a real intensity:

$$I^{nm}(x) = 2E_0^2 k_n^2 k_m^2 \cos \left\{ \frac{2\pi}{p} d_1 (n - m) \frac{\partial f(x)}{\partial x} + 2(\phi_n - \phi_m) \right\}$$
(15)

Note: all terms where  $n=m$  are background intensity terms.

$$\frac{\partial f(x)}{\partial x} = -2 \frac{\partial w(x)}{\partial x} \left( 1 + 2d_1 \frac{\partial^2 w(x)}{\partial x^2} \right)$$
(16)

Classically, the effect of curvature is neglected, and reflection Moiré patterns are analyzed considering the pattern as containing the slope only:

$$I^{nm}(x) = 2E_0^2 k_n^2 k_m^2 \cos \left\{ \frac{2\pi}{p} 2d_1 (n - m) \frac{\partial w(x)}{\partial x} - 2(\phi_n - \phi_m) \right\}$$
(17)

In order for this approximation to be reasonable, the curvature of the mirror must be very small, which makes the correction term negligible. The exact condition is:

$$2d_1 \frac{\partial^2 w(x)}{\partial x^2} \ll 1$$
(18)

or, defining  $R(x)$  as the local radius of curvature of the mirror:

$$|R(x)| \gg 2d_1$$
(19)

The resulting intensity  $I_T(x) = \sum_n \sum_m I^{nm}(x)$  is the summation of a number of cosine fringe patterns encoded with the slope of the surface. Each term  $(n,m)$  gives a pattern with a different sensitivity.

$$S_{mn} = 2 \left( d_1 \frac{(n - m)\lambda}{p} \right)$$
(20)

The fundamental harmonic is given by the lowest sensitivity, i.e. for  $|n - m| = 1$ . This corresponds to the interference between successive orders, for example (1,-1) (or (-1,1)) and (0,0):

$$I_f(x) = 2E_0^2 k_1^2 \cos \left\{ \frac{2\pi}{p} 2d_1 \frac{\partial w(x)}{\partial x} - 2\phi_1 \right\}$$
(21)

All other patterns are harmonics of this fundamental pattern. Furthermore, approximations of the derivative are varying in quality among these terms, since the greater the shear, the worse the approximation in (14). For this reason, the fundamental pattern is the most precise. Moreover, interference between shifted terms (( $n, -n$ ) and ( $n+1, -n-1$ ), for example, where  $n$  is not small) produce a shifted slope, so that the resulting pattern is a composite of shifted patterns.

However, the global pattern is of the form:

$$I(x) = I_0^* + I_1^* \cos \frac{2\pi}{p} \left( 2d_1 \frac{\partial w}{\partial x} \right)$$
(22)

although the shape is not exactly sinusoidal due to the presence of harmonics [10]. The first step in analyzing the Moiré pattern must therefore be filtering, to ensure that the fringes are truly cosine fringes.

#### IV. EXPERIMENTAL

The moiré reflection technique was applied to determine the curvatures of a real dental impression. The collimation of the light was

adjusted using a  $\lambda/20$  mirror. The position of the light source was adjusted so that no residual fringe can be observed in the field. Fig. 3 shows the steps to obtain the final shape reconstruction.

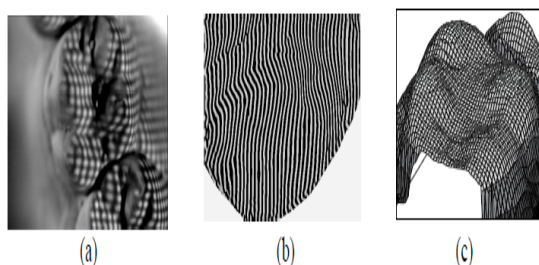


Figure 3: (a) grating projected on the specimen; (b) captured fringes; (c) shape reconstruction

The analysis of the reflection moiré fringes is performed by computer fringe analysis. The HOLOSTRAIN system [11] analyzes the fringes as spatially frequency modulated signals and determines the modulating function, extends the signal beyond the boundaries of the specimen and computes its derivative. In the case of in-plane deformation the modulating function is the displacement function of the points of the surface. In the case of Reflection Moiré, the modulating function is the slope function of the surface. The derivative of the function is the curvature [12]. The derivatives can be computed with a very high accuracy. In the particular examples shown in this paper, a grating of pitch 0.254 mm was used and the distance  $d_1$  was 300 mm. This means that sensitivities of  $1.2 \times 10^{-5}$  radians in the measurement of slopes can be achieved.

## V. CONCLUSION

The equations developed in this paper allow us to define a more accurate method for surface slope measurement. Through a new powerful automatic image analysis system, the whole shape of any kind of irregular surface can be reconstructed with very high precision.

## REFERENCES

- [1] Lichtenberg, F. K., "The Moiré method, a new experimental method for the determination of moments in small slab models," Proc. Soc. Exp. Stress Analysis, 2, Vol. 12, pp. 83-98, 1954-1955.
- [2] Rieder, G., Ritter, R., "Krummungsmessung an belasteten Platten nach dem Lichtenbergschen Moiré Verfahren," Forsch. Ing. -Wes. 2, Vol. 31, pp. 33-44, 1965.
- [3] Pedretti, M., "Nouvelle methode de Moiré pour l'analyse des plaques flechies," Doctoral Thesis, Ecole Polytechnique de Lausanne, 1974.
- [4] Richter, R., Herbst, M., "Ein Optisches System zur Aufnahme von Vermessungsgrossen dynamische belasteten Platten," Forsch. Ing. -Wes. 3, Vol. 42, pp. 82-85, 1974.
- [5] Chiang, F. P., Jaisingh, G., "A new optical system for Moiré methods, Exp. Mech., 11, Vol. 14, pp. 459-462, 1974.
- [6] Sciammarella, C. A., Davis, D., "Gap effect in Moiré fringes observed with coherent monochromatic collimated light," Exp. Mech., 8, Vol. 10, pp. 459-466, 1968.
- [7] Guild, J., "The interference system of crossed diffraction gratings," Chapter III, Oxford at Clarendon Press, 1956.
- [8] Sciammarella, C. A., "Use of gratings in strain analysis," Journal of Physics E. Scientific instruments, Vol. 5, pp. 833-845, 1972.
- [9] Sciammarella, C. A., Chang, T. Y., "Optical differentiation of displacement patterns using shearing interferometry wave front reconstruction," Exp. Mechanics, Vol. 11, 3, pp. 97-104, 1971.
- [10] Sciammarella C. A., Bhat, G., "Two dimensional Fourier transform methods for fringe pattern analysis," Proceedings of the VII international congress in Exp Mechanics, SEM, Vol. 2, pp. 1530-1538, 1992.
- [11] Sciammarella C., A. Yoshida S., Lamberti L., "Advancement of Optical Methods in Experimental Mechanics" SEM, Springer 2014.

[12] Sciammarella C. A., Sciammarella F. M.,  
“Experimental Mechanics of Solids” Wiley 2012.